Desalination and Water Treatment
www.deswater.com
doi: 10.1080/19443994.2015.1053530

57 (2016) 12453–12466
June

Taylor & Francis
Taylor & Francis Group

Application of the DYRESM–CAEDYM model to the Sau Reservoir situated in Catalonia, Spain

Saddek Takkouk[a,*], Xavier Casamitjana[b]

[a]*Département d'hydraulique, Université de Batna, 05000 Batna, Algeria, Tel. +213 796870130; Fax: +213 33816622; email: takkouks@yahoo.com*
[b]*Département de Physique, Université de Gérone, 17071 Montilivi, Gérone catalogne, Spain, Tel./Fax: +34 72 418379; email: xavier.casamitjana@udg.edu*

Received 19 March 2014; Accepted 15 May 2015

ABSTRACT

The aim of this work was to apply to the Sau Reservoir a one-dimensional hydrodynamic DYRESM model linked to the water quality CAEDYM model. And how hydrodynamic affects water quality in reservoirs, especially when have been used for water supply purposes. Thus, simulations were undertaken for 2 years between 2000 and 2001 with the aim of predicting thermal structure and water quality variables such as dissolved oxygen, dissolved inorganic phosphorus and chlorophyll in the reservoir. Inputs were meteorological data, river inflow and outflow data, morphometry parameters, an initial profile and file configuration data. The CAEDYM model also requires a configuration file and initial profiles for all the water quality data, as well as the calibration of different parameters such as sediment-dissolved oxygen, the sediment flux release rate of phosphorus and the maximum potential growth rate of phytoplankton. Temperatures simulation shows clearly a good agreement with the observed one during the stratification period starting from July to the end of September. Also, the model gives a good prediction of dissolved oxygen, however, for simulated dissolved inorganic phosphorus, and chlorophyll exhibits the same trend as measured values. Hence, coupling of those models explains in better way how water quality may be affected by hydrodynamic and could be used as an adequate tool for water quality management purposes.

Keywords: Hydrodynamic; Water quality; Calibration

1. Introduction

Most temperate lakes develop strong thermal stratification every summer. This stratification of the water column is due to differences in water density. In classical limnology, the water column can be divided into three layers: epilimnion, metalimnion and hypolimnion, although many Mediterranean lakes present a continuously stratified profile. Chemical and biological gradients reflect the thermal stratification, which is mainly affected by external forces such as heat input, wind velocity and lake morphometry. The stratification magnitude also depends on the river inflow temperature [1]; the River Ter, the Sau's main tributary, is polluted and contains a high concentration of nutrients, mainly ammonia and soluble reactive phosphorus [1], but also particulate and dissolved organic matter. The inflow temperature is usually lower than the reservoir's surface layer and therefore the water sinks to the depth

*Corresponding author.

at which its density is equal to that of the reservoir water at that level. The inflow water is characterized by a higher flow velocity, and consequently, causes thermocline erosion. Additionally, inflow is one of the main sources of nutrients and other chemical materials entering a reservoir, and its intrusion can influence the vertical gradient of nutrients.

Several hydrodynamic and water quality models have been developed to study the seasonal dynamics amid these models; a simple empirical model that has been developed since the mid-1960s to predict eutrophication on the basis of the phosphorous (P) loading concept [2], see reviews by Mueller [3] and Ahlgren et al. [4]. Afterwards, other models have been developed following this approach. Examples include AQUASYM by Kmeť et al. [5] and Karagoumis et al. [6]. Finally, an approach that has been developed by 1D hydrodynamic model to include water quality parameters such as DLM-WQ, MINILAKE by Riley and Stefan [7], DYRESMWQ [8], and 1-D, 3-D Dynamic Reservoir Simulation Model DYRESM, ELCOM coupled with an ecological model CAEDYM; these last two models were developed in water centre of the Western University of Australia.

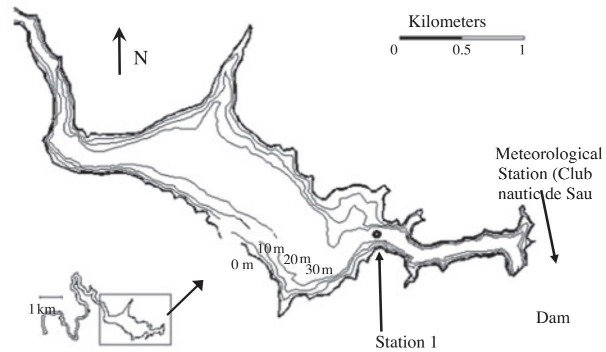

Fig. 1. Bathymetric map of the Sau Reservoir showing the location of measuring stations and the meteorological station.

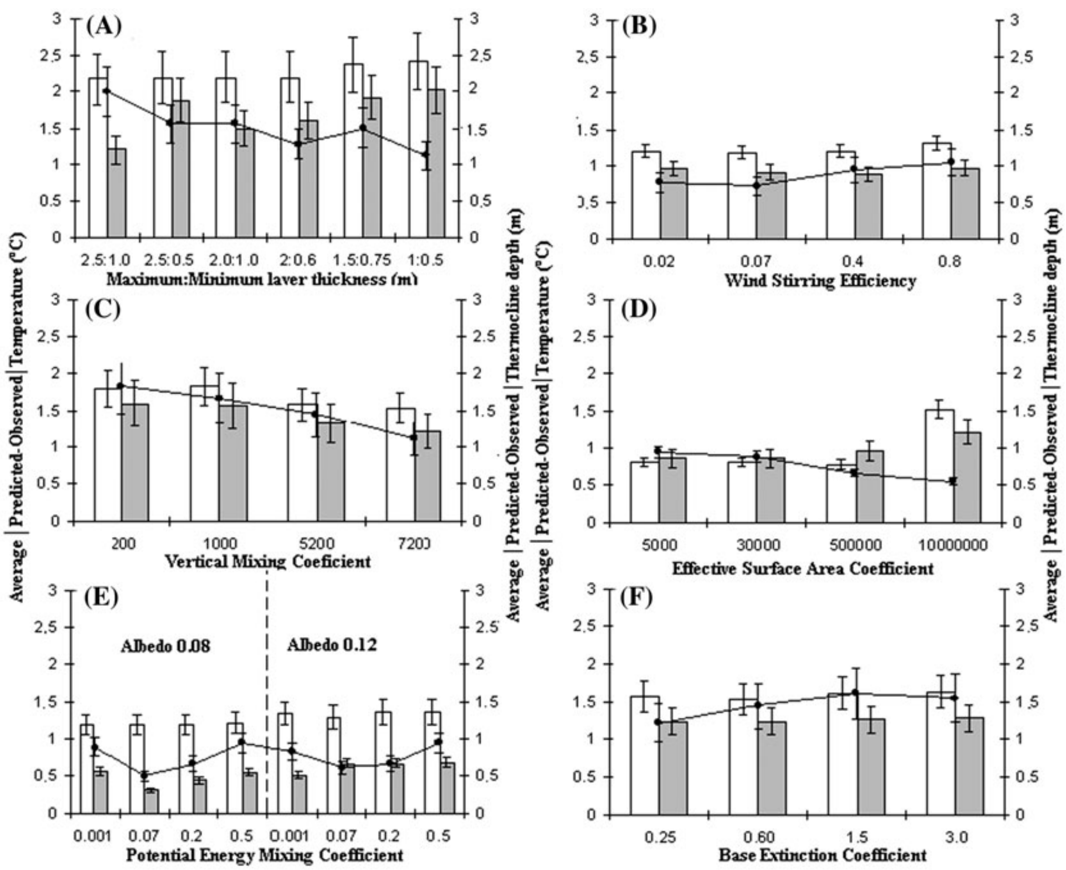

Fig. 2. Average absolute difference ± standard error of the mean between DYRESM–CAEDYM predicted and observed water temperatures (white), bottom water temperature (grey) and thermocline depth (line) at various layer thickness settings (A), wind stirring efficiency values (B), vertical mixing coefficient (C), effective surface area coefficient (D), albedo and potential energy mixing coefficient values (E) and base extinction coefficient (F).

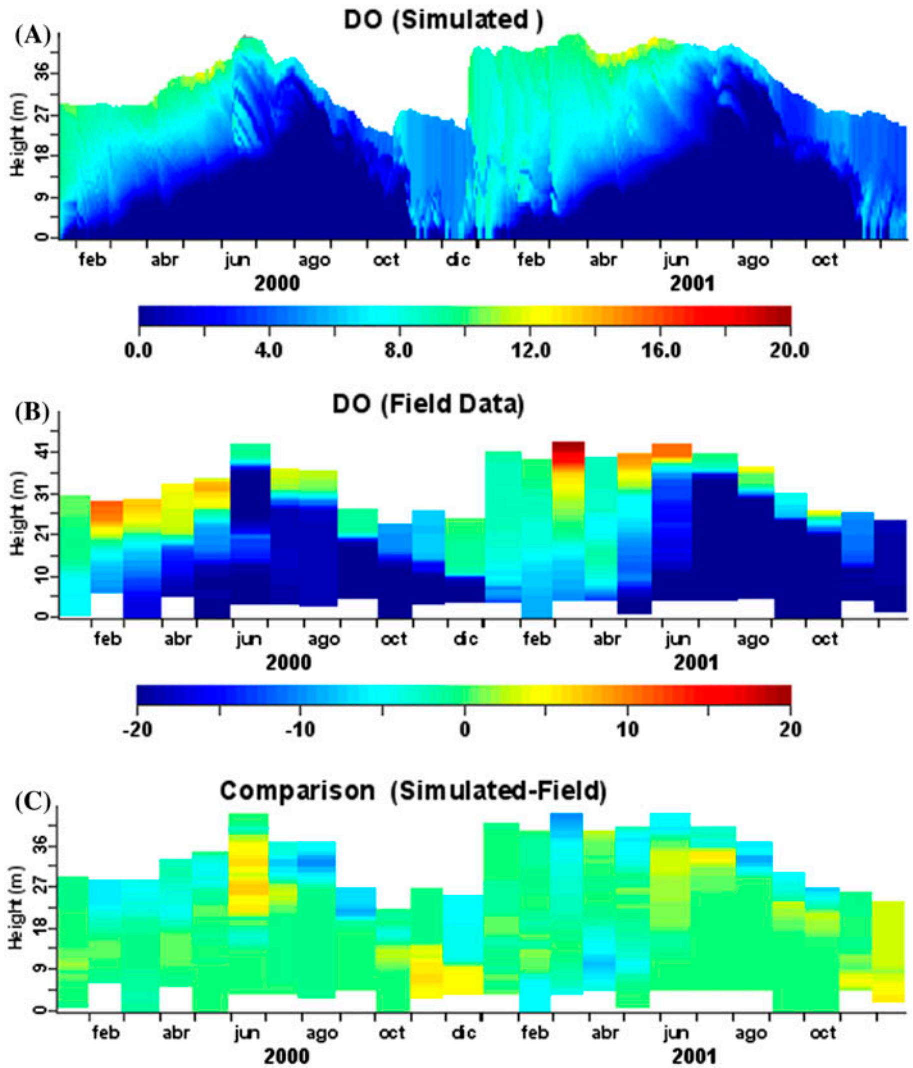

Fig. 3. Two years (2000–2001): simulated dissolved oxygen (A), measured dissolved oxygen (B) and comparison (C).

A coupled hydrodynamic and ecological water quality model DYRESM–CAEDYM is the significant advance on previous models that seeks to predict water quality in lakes and reservoirs and has been used several times for Sau Reservoirs by most of the researchers. The DYRESM–CAEDYM combines a one-dimensional hydrodynamic model with a water quality model to predict thermal structure and water quality variables such as dissolved oxygen, dissolved inorganic phosphorus and chlorophyll. We calibrate it for the dry year 2001 and validate it for the year 2000.

2. Materials and methods

The Sau Reservoir is the first of a cascade of reservoirs situated in the central part of the River Ter, which was first filed in 1964. The River Ter is 200 km long and has its source in the Pyrenees in the NE of Spain. One of the most characteristic feature of Sau, a river valley reservoir 18.225 km long, is its canyon-shaped morphology (Fig. 1). The length of the lacustrine part of the reservoir is 3,600 m and its maximum width is 1,300 m [9]. The use of the Sau Reservoir water as a drinking water supply to the Barcelona metropolitan area explains why it has been studied ever since it was first used for this purpose. As [1] has shown, the Sau's trophic condition has evolved in response to human activity in the watershed overtime, in particular in terms of the presence of soluble reactive phosphorus and inorganic dissolved nitrogen. Following the construction of sewage treatment plants, the phosphorus has

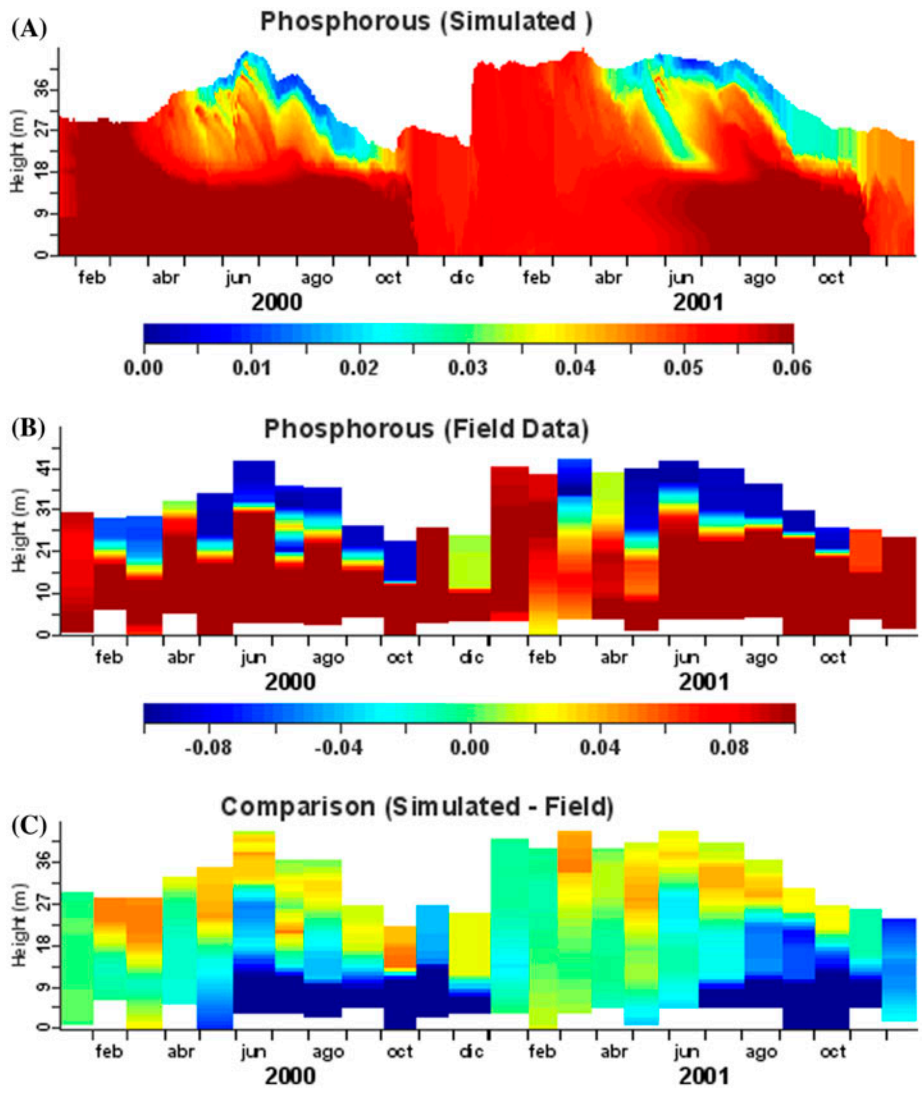

Fig. 4. Two years (2000–2001): simulated dissolved inorganic phosphorus (A), measured dissolved inorganic phosphorus (B) and comparison (C).

decreased, but the dissolved inorganic nitrogen has increased. We are attempting to study the hydrodynamics and water quality of the Sau Reservoir for 2000–2001. The available data were supplied by a team led by professor Armengol. Temperature calibration has been done by varying minimum and maximum layer thickness as [10] has found. Additionally, in our study, we found out that also vertical mixing coefficients and effective surface area are very important calibration parameters.

3. DYERESM–CAEDYM calibration and validation

DYRESM–CAEDYM [11,12] was configured during two years period from 2000 to 2001 to simulate temperature and water quality parameters such as dissolved oxygen, nutrients, and chlorophyll for Sau Reservoir. Simulation start date was chosen as the nineteenth of January 2000, for which first temperature profiles were recorded.

The calibration process of the model is required because biological systems are inherently different. As a first step, we calibrate the model for the year 2001 which was a dry year. After that, we validate the model for the year 2000. It should be noted that the inflow file in the ecological model must include daily water quality concentration data as well as daily temperature and salinity.

The lack of daily river water quality data such as dissolved oxygen, dissolved inorganic phosphorus and chlorophyll makes the simulation impossible unless hypothetical data is used.

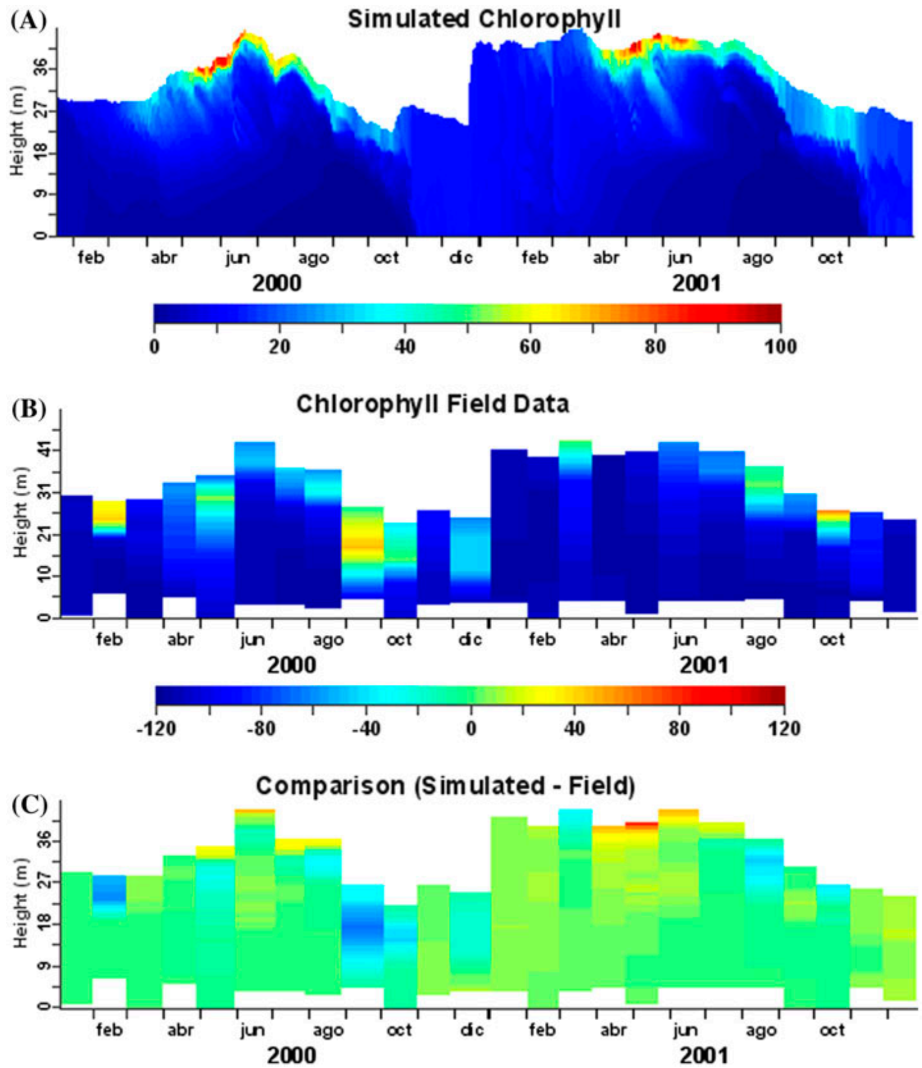

Fig. 5. Two years (2000–2001): simulated chlorophyll (A), field chlorophyll (B) and difference (C).

Our hypothesis concerning daily water quality had to be estimated from available reservoir water profiles means nutrient inflow concentrations have to be estimated from reservoir water profiles as the long-term mean of the in-lake concentrations which we take as the inflow nutrient data constant over the entire simulation period. In our study, the CAEDYM model was configured to simulate the dynamics of dissolved oxygen, dissolved inorganic phosphorus and one phytoplankton group. However, in the hydrodynamic model, DYRESM's several input parameters implicated in the thermal processes were tested for their influence on heating and mixing in the DYRESM model. So, varying wind speed using a wind factor multiplier of 1.3 and 1.5 does not give a substantial variation in the predicted thermal structure, probably due to the weak wind velocity registered in 2000 and 2001. Only changes in benthic boundary layer thickness from 0 to 0.02 resulted in a slight difference in surface water temperatures. However, tested parameters, such as minimum and maximum layer thickness, vertical mixing coefficient, effective surface area, wind stirring coefficient potential energy mixing and base extinction coefficient produced acceptable changes in predicting water temperature profiles. So minimum and maximum layer thickness, diffusive fluxes constant and effective surface area were designated as highly sensitive parameters. Thus, six separate calibrations were performed, the first for the layer thickness and the second for the wind stirring efficiency parameter, to identify the values of these parameters in calibration process which would result in the least

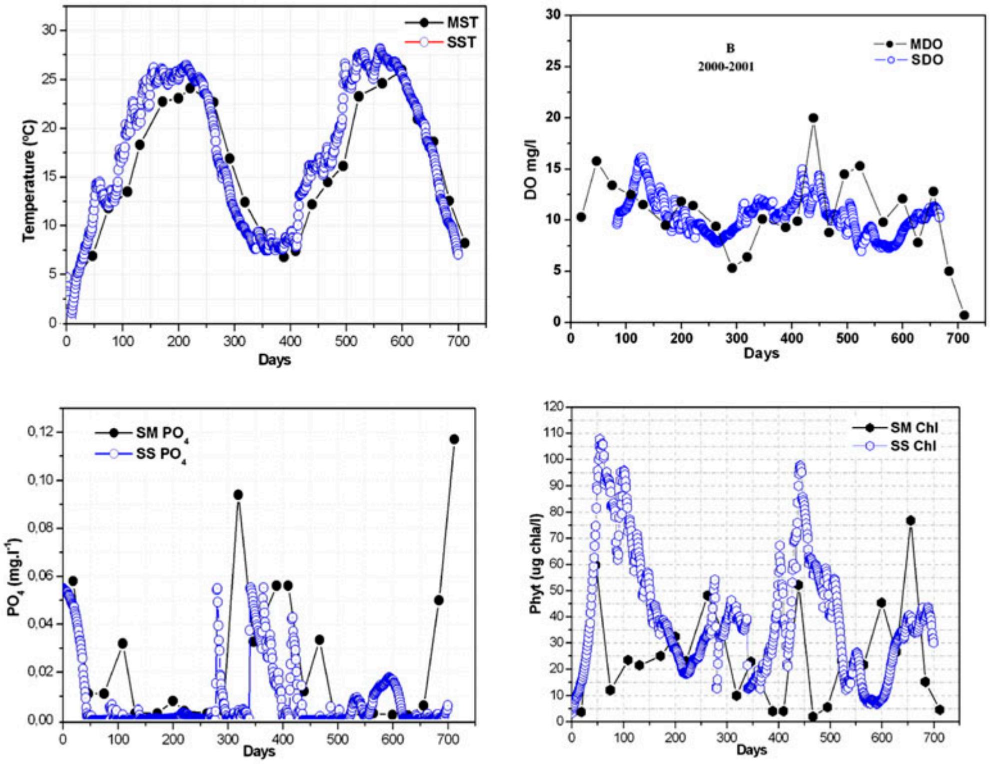

Fig. 6. Comparison between water surface simulation (open circles) and observation (filled circles) of temperature (A), dissolved oxygen (B), phosphorus (C) and chlorophyll (D).

amount of error between observed and predicted temperature profiles. Minimum layer thickness varied between 0.5, 0.6, 0.75 and 1.0 m and maximum layer thickness between 1, 1.5, 2.0 and 2.5. For the calibration of layer thickness, all simulations involved maximum layer thickness set to equal or less than twice the minimum layer thickness. The second calibration is the wind string efficiency which testing values are 0.8, 0.4, 0.07, and 0.02.

The third setting is the vertical mixing coefficient which has testing values of 200, 1,000, 5,200, and 7,200 with reference to the adequate values of minimum layer thickness, maximum layer thickness and wind stirring efficiency values identified in the preceding calibration.

Fourth setting is an effective area coefficient, the tested values area are 5,000, 30,000, 500,000 and 10,000,000; fifth is the base extinction coefficient with value varying between 0.25, 0.6, 1.5 and 3.0, and finally, setting the values of potential energy mixing coefficient at 0.001, 0.07, 0.2 and 0.5 at albedo values of 0.08 and 0.12, respectively.

A maximum layer thickness of 1.5 m and minimum layer thickness of 0.5 m were the best settings to predict water temperature at all depths (Fig. 2(A)) as was described by Andrew et al. [10]. The simulation also demonstrated that wind stirring efficiency parameter of 0.07 performed well as predictors of water temperature, bottom temperature T_B and thermocline depth Z_T (Fig. 2(B)). However, we admit a value of 0.06 to remain consistent with the recommendation in the DYRESM operating literature [13] which wind stirring efficiency was estimated to 0.06.

An increase in the vertical mixing coefficient tends to decrease in the differences between predicted and observed temperature W_T, predicted and observed bottom temperature T_B, and predicted and observed thermocline depth Z_T (Fig. 2(C)). Thus, the best value was 7,200. Effective surface area, giving the best thermocline depth Z_T, was a value of 1×10^7, but corresponding at high difference between predicted and observed water temperature and bottom temperature W_T and T_B (Fig. 2(D)).

Base light extinction coefficient only decreases the difference between predicted and observed thermocline temperature and have no influence to the water temperature and bottom temperature (Fig. 2(F)). Finally, the simulations demonstrated that thermocline depth was less accurately predicted than at lower

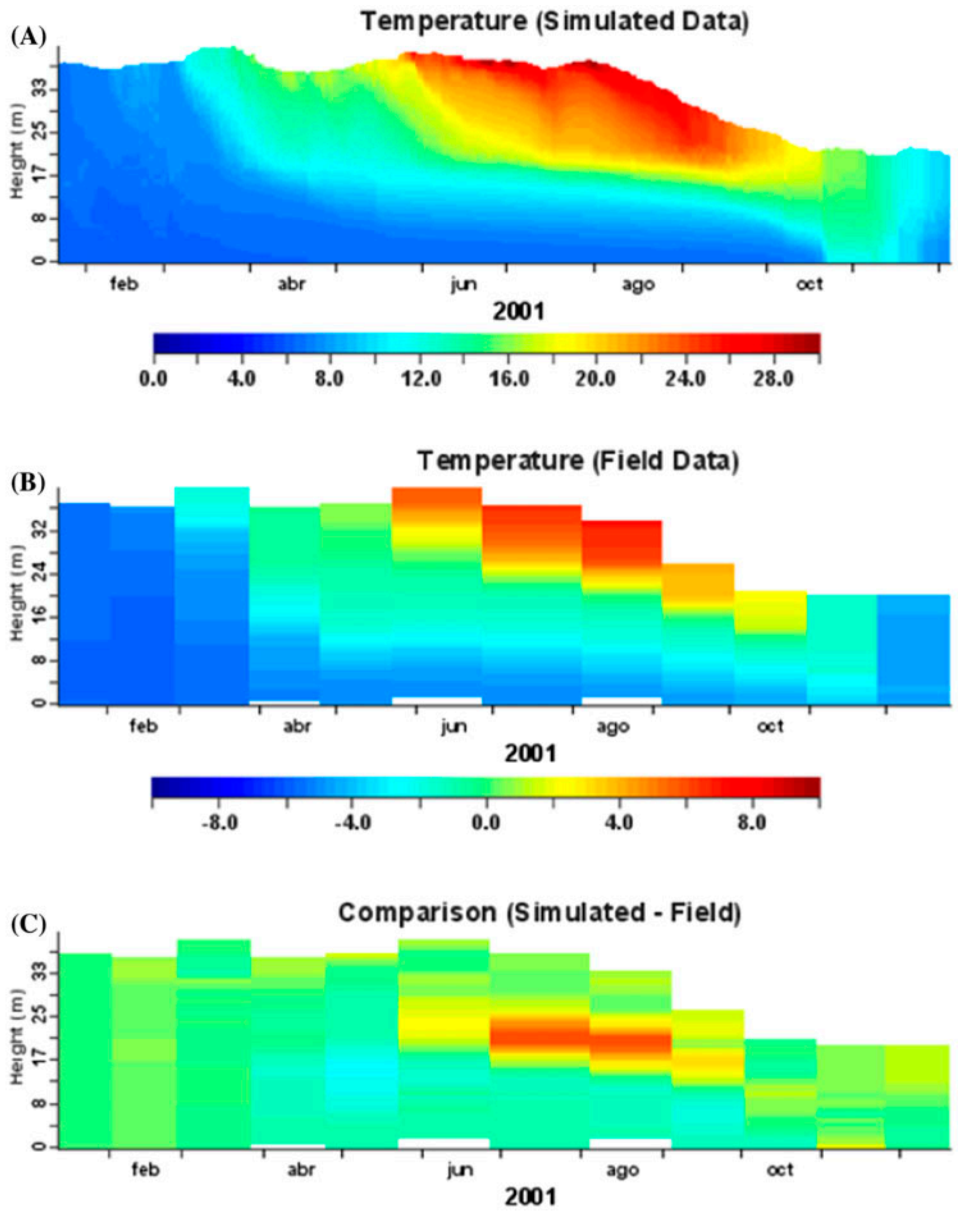

Fig. 7. One year (2001): simulated temperature (A), measured temperature (B) and difference between simulated and measured (C).

albedo. Whereas, an increase solely in albedo increased the differences between predicted and observed temperatures as well as differences between predicted and observed bottom temperature (Fig. 2(E)). Table 1 summarizes sensitive and insensitive parameters in the model.

The ecological model was calibrated by trial-and-error adjustment of the most sensitive water quality parameters to give the best match with trends in the field, meaning that the calibration process has to start with temperature, dissolved oxygen, phosphorus and finally with the chlorophyll. After temperature calibration, the mean sensitive parameters in dissolved oxygen are static dissolved consumption by sediments and half saturation constant for sediment oxygen demand, and the principal parameters in phosphorus calibration are maximum rate of phytoplankton phosphorus uptake and the sediment flux release rate of phosphorus, and the parameters that affect chlorophyll are growth rate, phosphorus and light utilization. The water quality calibration parameters are grouped in Table 2.

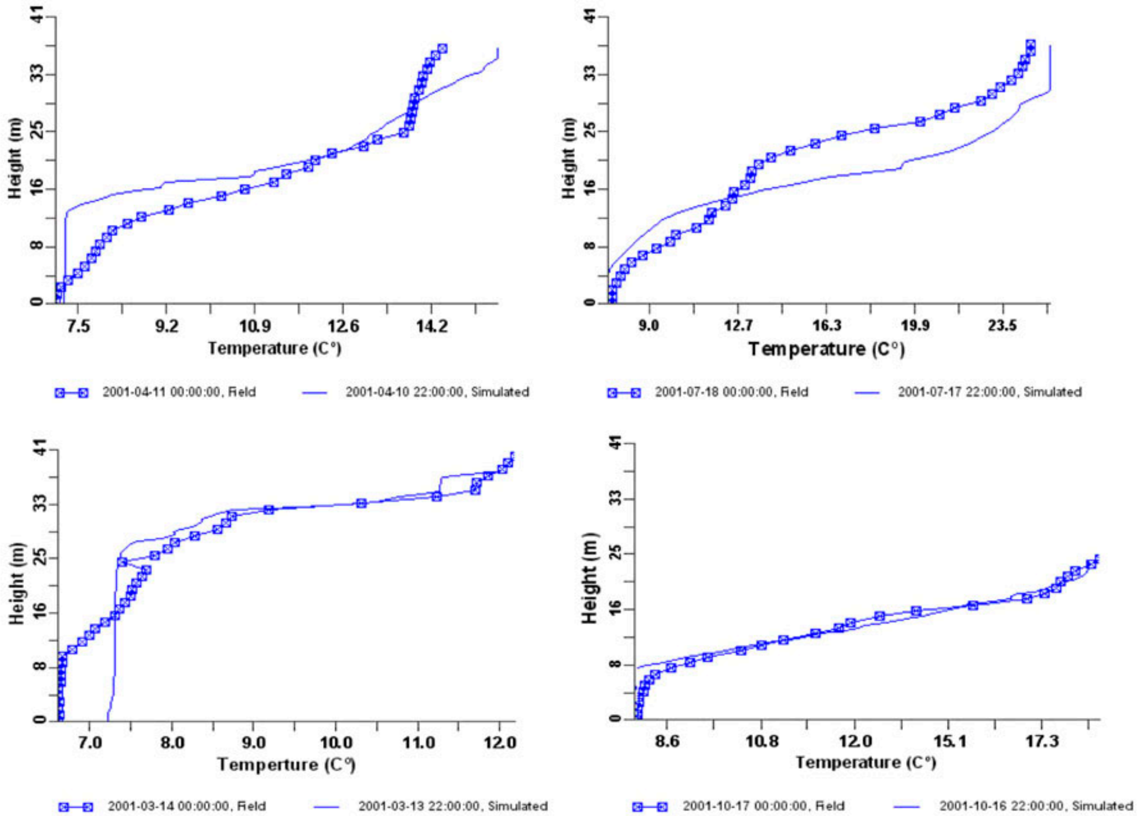

Fig. 8. Comparison of temperature profiles between observed and simulated results on four Julian days: 44, 101, 199 and 290 of the year 2001. Squares represent the observed results, and the lines represent the simulations.

As previously stated, the calibration period was assigned to the dry year from 23 January 2001 to 13 November 2001.

Calibration of dissolved oxygen requires checking of the sediment oxygen demand, the organic contribution and the inflow concentration. The calibration of dissolved inorganic phosphorus depends on the inflow concentration, the sediment release rate, inorganic particulates, phytoplankton as it was described by Aminot and Kérouel [14], and finally, chlorophyll, which is the most difficult parameter to calibrate because it depends on the information that is available about modelled species such as growth rate, nutrients, light utilization and settling or vertical migration characteristics. The overall calibrated parameters are grouped in Table 2.

After calibration, the DYRESM–CAEDYM model is used to simulate reservoir behaviour over 705 d, from 19 January 2000 to 31 November 2001, a 2-year period that includes the 1-year calibration period. It will be seen later that there is strong density stratification during the warmer months of the year. Simulated dissolved oxygen concentrations will demonstrate the existence of an anoxic zone in the deeper hypolimnion during the stratification period. Phosphorus simulation will also show an important load of this nutrient at the bottom of the hypolimnion. For chlorophyll, the simulation will show the existence of algal blooms on the surface. The 2-year series of simulated temperature, dissolved oxygen, phosphorus and chlorophyll compared to field series are shown in Figs. 3–6.

4. Results and discussion

Using daily averaged short-wave radiation, long-wave radiation, wind speed, inflow/inflow temperature and withdrawal from 2000 to 2001 as input data, a good agreement was found between the simulated and observed temperatures measured at the Nàutic station. For the year 2001 (Fig. 7), the agreement is especially good for the period ranging from January to July, and during the autumn, the maximum difference observed was 1°C. However, during the stratification period running from July to the end of September, the simulated temperature in July and August was higher than the observed, especially at a depth of 20–25 m. The maximum observed difference

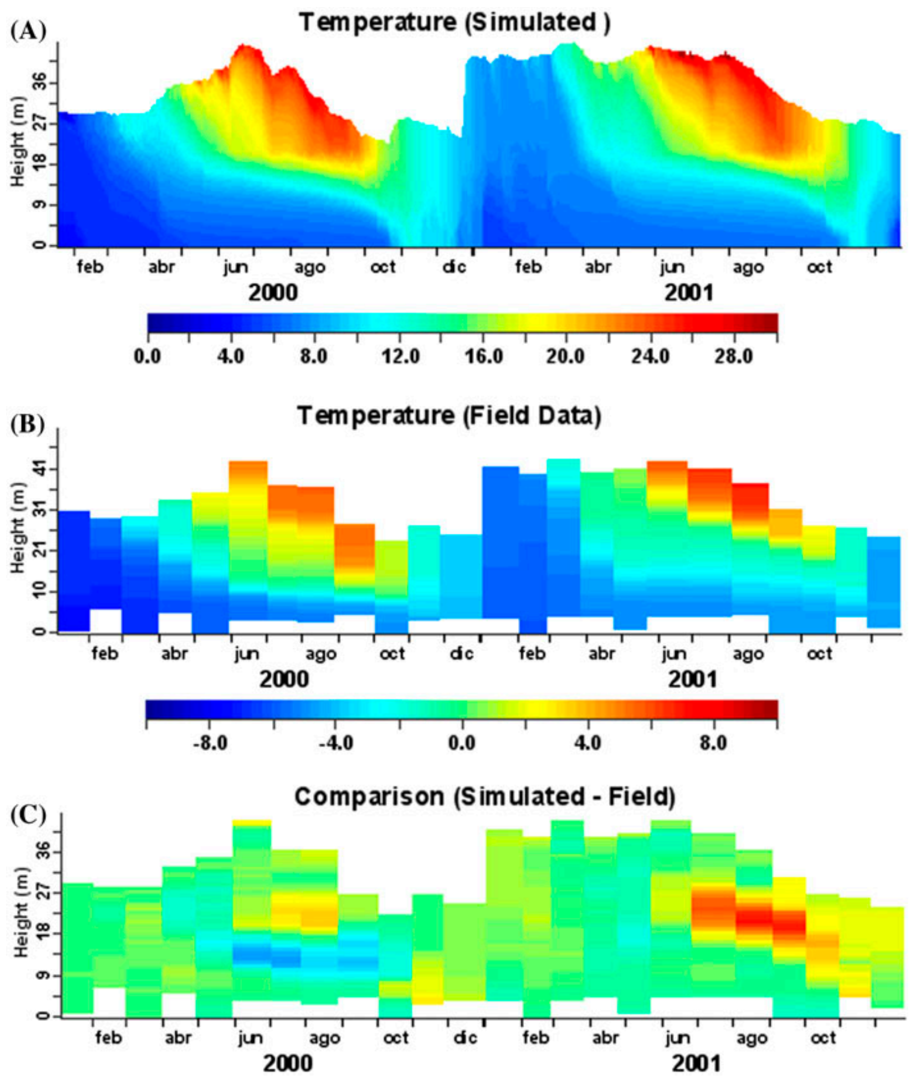

Fig. 9. Two years (2000–2001): simulated temperature (A), measured temperature (B) and comparison (C).

was 4.5˚C. In the surface layer (Fig. 6(A)), simulated temperatures fit well with the observed ones.

For comparison purposes, we chose four profiles on Julian days 44, 101, 199 and 290 because they represent four seasons in the year 2001. In Fig. 8, the difference between simulated and observed profiles is presented. On Julian day 44, the simulated bottom temperature is about 0.5˚C lower than the observed, and on Julian day 101, the simulated hypolimnetic temperature is approximately 1˚C higher than the observed.

However, the epilimnion temperatures taken during the same day show an inverse tendency. For Julian day 199, there is a small difference between simulated and observed temperatures in the surface mixed layer, and for Julian day 290, simulated and observed temperatures are very similar. The simulated metalimnetic temperature is higher than the observed one of Julian days 44 and 101. The opposite is the case of Julian day 199, but the simulated temperature is approximately the same as the observed one for Julian day 290.

In Fig. 7, the temperature isolines are more separated in the observed than in the simulated data (see also Fig. 9) meaning that the predicted metalimnion is higher than the reality. This may be due to two-dimensional effects such as higher internal mode waves not taken into account in a 1D model [13], or due to the fact that metalimnetic mixing in the DFYR-ESM model is stronger than in reality. In spite of this, the comparison between simulated and observed temperatures shows that the DYRESM–CAEDYM model can be accepted as a good tool for predicting the evolution of the thermal cycle in the Sau Reservoir.

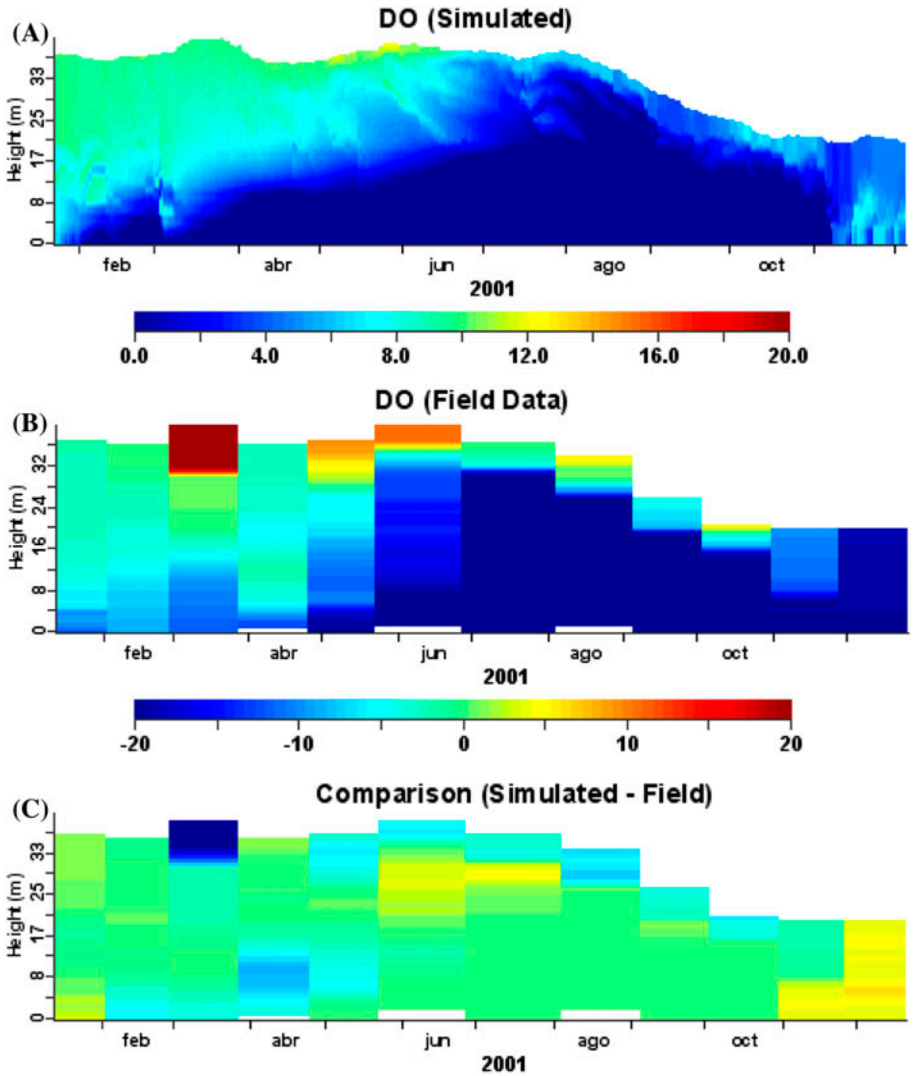

Fig. 10. One year (2001): simulated dissolved oxygen (A), observed dissolved oxygen (B) and comparison (C).

Table 1
Values of coupled model parameters and model simulation specifications

Parameter set value albedo	0.08
Benthic boundary layer thickness (m)	0.00
Bulk aerodynamic momentum transport coefficient	0.0013
Critical wind speed (m s^{-1})	3.0
Effective surface area coefficient	1.0×10^7
Emissivity of a water surface	0.96
Non-neutral atmospheric stability correction switch	No
Potential energy mixing efficiency	0.20
Shear production efficiency	0.08
Vertical mixing coefficient	200
Wind stirring efficiency	0.06
Following calibrations	
Minimum layer thickness	0.5 m
Maximum layer thickness	1.5 m
Effective surface area coefficient	1×10^7
Vertical mixing coefficient	7,200

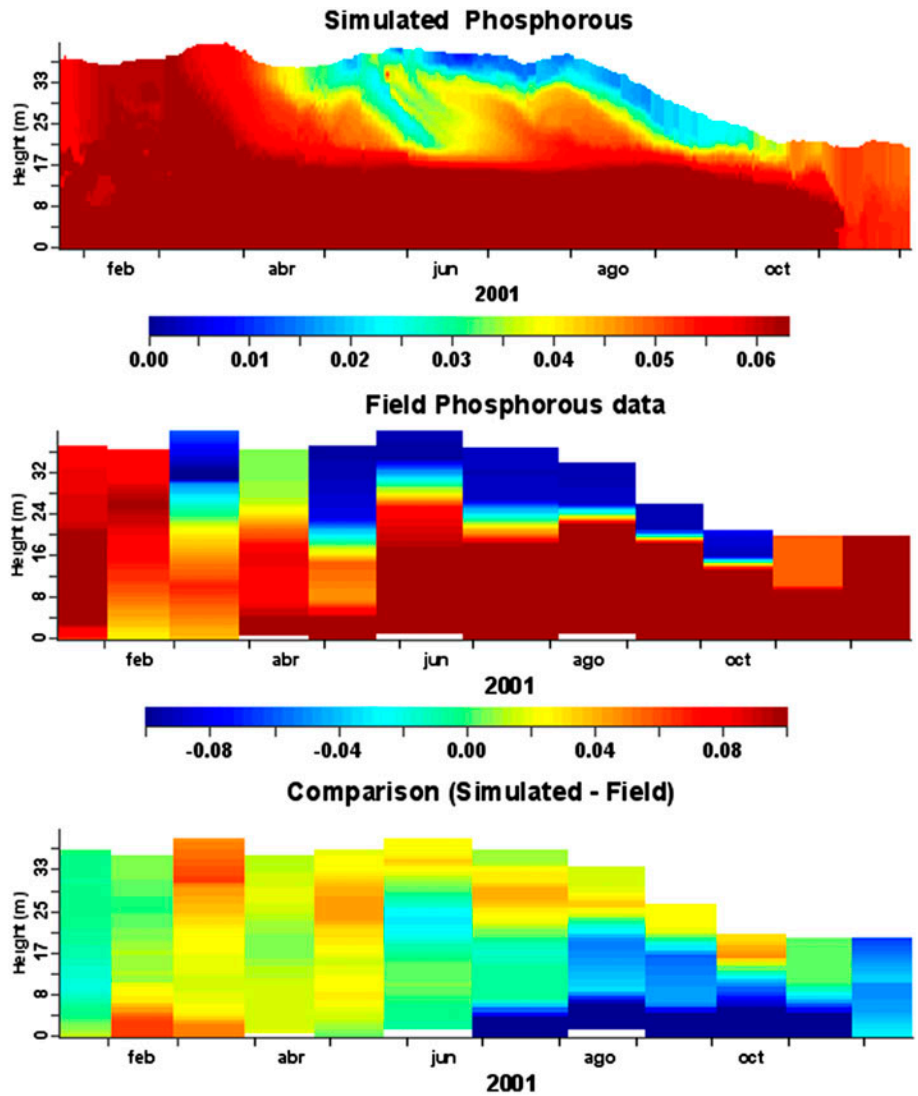

Fig. 11. One year (2001): simulated dissolved inorganic phosphorus (A), measured dissolved inorganic phosphorus (B) and comparison (C).

The simulated dissolved oxygen concentrations in Fig. 10(A) are in reasonable agreement with the field measurements. Simulated dissolved oxygen concentrations in Figs. 10(A) and 3(A) give a good prediction of dissolved oxygen represented in the depletion of the reservoir's hypolimnion. The concentration of dissolved oxygen is in the range of 0–4 mg l^{-1}. This lower DO concentration promotes anaerobic processes and produces gases such as methane, hydrogen sulphide and ammonia. These gases impart a bad taste to drinking water and in large concentrations can be toxic. Therefore, it is necessary to intervene quickly using a destratification system to maintain water quality standards. The high amount of dissolved oxygen measured in the surface layer's March profile (18 mg l^{-1}) (see Fig. 6(B)) is probably due to a peak in the level of bloom algae, most likely diatoms, in early spring, which the model cannot reproduce. From January to March 2001, there is a deficit (5 mg l^{-1}) of dissolved oxygen in the bottom layer, despite the mixing in this period. The reason is that the deeper hypolimnion is not totally mixed. However, from the end of October 2001 until the end of the same year, the opposite occurs: simulated dissolved oxygen is a little higher than that in the field; the difference is estimated at (5 mg l^{-1}).

In general, though, it can be said that the DYERSM–CAEDYM model is a good predictor of dissolved oxygen in the Sau Reservoir in spite of the anomalies described above.

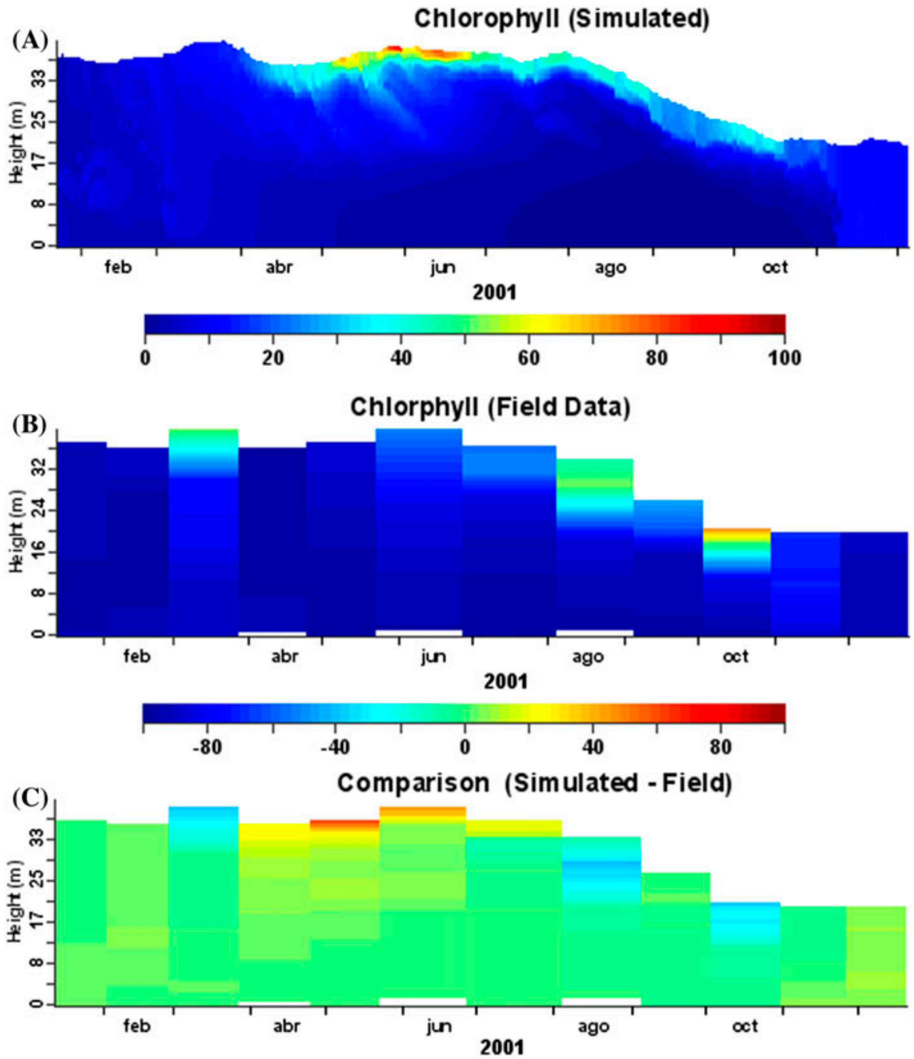

Fig. 12. One year (2001): simulated chlorophyll field chlorophyll (B) and comparison (C).

The simulated dissolved inorganic phosphorus concentration displayed in Figs. 11(A) and 4(A) exhibits the same trend as the concentration that was measured. A high phosphorus concentration at the bottom and depletion in the surface layer were observed during the stratification period, which indicates that this element is probably the main factor of biological activity in the Sau Reservoir. Also, mixing occurred in winter and autumn. So, we can say the model gives a good prediction of the phosphorus for half of the year 2001. Nevertheless, from time to time, we observe a simulated phosphorus concentration that is high compared to that observed in the field, which is perhaps due to the river inflow phosphorus concentration. On the other hand, for the second half of the same year, there is a big deficit between simulated and observed phosphorus concentrations, especially in the hypolimnion (see Figs. 11(C) and 4(C)). The reason is still unclear, but the excess of phosphorus on the bottom layer in the field may be due to an extra source of phosphorus that has not been taken into account, such as ground water flow, or to illegal seepage of agricultural sewage water, infiltrating directly from the catchment area into the reservoir and bypassing treatment plants. It appears that the DYRESM–CADYM model simulates dissolved inorganic phosphorus in the surface layer well (Fig. 6(C)) and accurately represents trends elsewhere in the field. However, the big difference between the field and simulations in the bottom layer may depend on the accuracy of data. The neglect of lateral and longitudinal phosphorus concentrations may also impact on the simulation.

With regard to chlorophyll, the DYRESM–CAEDYM model's simulation correctly indicates the

Table 2
The major calibrated water quality parameters used in the DYRESM–CAEDYM model

Parameter	Description	Units	Assigned range	Assigned value
Dissolved oxygen				
ϑ_{op}	Temperature multiplier for SOD	–	1.02–1.14	1.07
F_{SOD}	Static sediment exchange rate	$g\ m^{-2}\ d^{-1}$	0.02–15	3.2
K_{SOD}	½ sat constant for static DO sediment	$mg\ DO\ l^{-1}$	–	0.2
ϑ_{ON}	Temperature multiplier for nitrification	–	1.001–1.10	1.08
k_n	Nitrification rate coefficient	d^{-1}	0.01–0.1	0.02
K_N	Half saturation constant for nitrification	$mg\ DO\ l^{-1}$	–	2.0
k_r	Phytoplankton respiration mortality/excretion	d^{-1}	0.01–0.10	0.08
K_{DOB}	Half sat const for DO dependence of POM/DOM decomposition	$mg\ DO\ l^{-1}$	–	3.0
Dissolved inorganic phosphorus				
IP_{min}	Minimum phytoplankton internal phosphorus	$mg\ P(mg\ ChIa^{-1})$	0.1–1.0	0.6
IP_{max}	Maximum phytoplankton internal phosphorus	$mg\ P(mg\ ChIa^{-1})$	1.0–5.0	2.2
UP_{max}	Maximum rate of phytoplankton phosphorus uptake	$mg\ P(mg\ ChIa^{-1})\ d^{-1}$	0.05–1.0	0.2
K_{ep}	Specific attenuation coefficient (phytoplankton)	$\mu g\ Chlal^{-1}\ m^{-1}$	–	0.016
K_{ePOC}	Specific attenuation coefficient of POC (particles)	$mg\ m\ l^{-1}$	–	0.001
POP_{1max}	Maximum transfer of POPL→DOPL (decomposition)	d^{-1}	–	0.2
DOP_{1max}	Maximum mineralization of DOPL→PO_4 (mineralization)	d^{-1}	0.01–1.0	0.075
DOP_{2max}	Maximum mineralization of DOPR→PO_4 (mineralization)	d^{-1}	0.002–0.018	0.003
S_p	Sediment flux release rate of phosphorus	$g\ m^{-2}\ d^{-1}$	3.10^5–8×10^5	5×10^5
K_P	Half saturation constant for phosphorus	$mg\ l^{-1}$	0.001–0.025	0.005
ϑ_S	Temperature multiplier of sediment fluxes	–	1.001–1.10	1.05
Chlorophyll				
P_{max}	Maximum potential growth rate of phytoplankton	d^{-1}	1.3–3.5	1.3
ϑ_p	Phytoplankton temperature multiplier	–	1.02–1.14	1.06
I_{KI}	Parameter for initial slope of P_I curve	$\mu Em^{-2}\ s^{-1}$	100–500	100

existence of phytoplankton blooms at the surface level since early spring, as shown in Figs. 12(A) and 5(A). However, in the simulation, theses blooms extend to July with a high order of magnitude compared to what was observed (Fig. 6(D)). The probable cause is the existence of one or more different phytoplankton species as diatoms which we have not been considered. As it was described by Serra et al. [15,16], green algae, diatoms and cryptophyceae where the dominant phytoplankton community in the summer period. Therefore, inclusion of S_i dynamics into CAEDYM may reduce the algal biomass peak via limitation by this third macronutrient, as well as the limitations of the one-dimensional model may be the cause of this difference. As it was described by Vidal et al. [17], in March and August, the simulated and observed levels are far apart. Chlorophyll is, therefore, seen to be very difficult to calibrate because it depends on all the variables described above, and any changes in their calibration factors affect its concentration.

5. Conclusion

The DYRESM–CAEDYM model requires daily inflow data concerning temperature and dissolved oxygen, nutrient and chlorophyll concentrations. However, where there is a lack of real measurements of these concentrations, it is acceptable to allow hypothetical data. Our hypothesis is based on the idea of using variable reservoir profiles to deduce daily concentrations throughout the simulation period. So, daily phosphorus and chlorophyll concentrations were considered as the long-term mean of the in-lake concentrations. Following a long calibration and validation process, we can say that the DYRESM–CAEDYM model is a useful tool to aid the understanding of hydrodynamic, nutrient and phytoplankton dynamics.

In general, the model reflects reality in terms of temperature and dissolved oxygen measurements and gives a general view of trends in phosphorus and chlorophyll concentrations. Obviously, it would not be realistic to expect a perfect fit to the observed data, so we have to accept some uncertainty. Unfortunately, the differences between the simulated and observed measurements, especially for phosphorus and chlorophyll, can be linked to many different factors, such as data accuracy, inflow water nutrient and chlorophyll concentration data, the neglect of certain parameters such as groundwater and the limits of the one-dimensional assumption [18]. Some types of phytoplankton are not taken into account in our modelling that could interfere and have a negative effect on the simulation, especially when modelling chlorophyll, could also be responsible. But in the end, the DYRESM–CAEDYM model is adequate for predicting the hydrodynamic and water quality of Mediterranean reservoirs, especially if further monitoring of the catchment area, rivers, is enhanced. Therefore, it will be an advantage to produce high-quality results which are subordinate to be done by close cooperation between modellers and field researchers. Aftermath, it could be used to allow water resources managers to predict how will to respond to changes in water quality management regimes and environmental factors.

Acknowledgement

The author acknowledges the PhD scholarship provided by IGSOC, University of Girona, Catalonia, Spain, that has resulted in this article.

References

[1] J. Armengol, J. Toja, A. Vidal, Seasonal rhythm and secular changes in Spanish reservoirs, in: R. Margalef (Ed.), Limnology Now: A Paradigm of Planetary Problems, Elsevier Science, Amestrdam, 1994, pp. 237–253.
[2] R.A. Vollenweider, The scientific basis of Lake Eutrophication, with particular reference to phosphorus and nitrogen as eutrophication factors. Tech. Rep. DAS/DSI/68.27, OECD, 1968, 159pp.
[3] D.K. Mueller, Mass balance model estimation of phosphorus concentrations in reservoirs, Water Res. Bull. 18(3) (1982) 377–382.
[4] I. Ahlgren, T. Frisk, L. Kamp-Nielsen, Empirical and theoretical models of phosphorus loading, retention and concentration vs. lake trophic state, Hydrobiologia 170 (1988) 285–303.
[5] T. Kmeť, M. Straškraba, P. Mauersberger, A mechanistic model of the adaptation of phytoplankton photosynthesis, Bull. Math. Biol. 55(2) (1993) 259–275.
[6] I. Karagounis, J. Trösch, F.A. Zamboni, A coupled physical-biochemical lake model for forecasting water quality, Aquat. Sci. 55(2) (1993) 87–102.
[7] M.J. Riley, H.G. Stefan, Minilake: A dynamic lake water quality simulation model, Ecol. Model. 43 (1988) 155–182.
[8] D.P. Hamilton, S.G. Schladow, Prediction of water quality in lakes and reservoirs. Part I—Model description, Ecol. Model. 96 (1997) 91–110.
[9] J. Armengol, J. Gracia, M. Comerma, M. Romero, J. Dolz, M. Roura, B.P. Han, A. Vidal, K. Simek, Longitudinal processes in canyon type reservoirs: The case of Sau (N.E. Spain), in: J.G. Tundisi, M. Straskraba (Eds.), Theoretical Reservoir Ecology and its Applications, Backhuys Publishers, Leiden, 1999, pp. 313–345.
[10] A.J. Tanentzap, D.P. Hamilton, N.D. Yan, Calibrating the Dynamic Reservoir Simulation Model (DYRESM) and filling required data gaps for one-dimensional thermal profile predictions in a boreal lake, Limnol. Oceanogr. Methods 5 (2007) 484–494.
[11] J. Antenucci, A. Imerito, The CWR Dynamic Reservoir Simulation Model DYRESM. Science Manual. Centre for Water Research, University of Western Australia, Perth, 2002.
[12] M.R.J. Hipsey, R. Romero, J.P. Antenucci, D. Hamilton, Computational Aquatic Ecosystem Dynamic Model: CAEDYM v2 Science Manual, Center for Water Research, University of Western of Australia, Perth, 2005.
[13] J. Antenucci, A. Imerito, The CWR Dynamic Reservoir Simulation Model DYRESM. User Manual, Centre for Water Research, University of Western Australia, Perth, 2003.
[14] A. Aminot, R. Kérouel, Dissolved organic carbon, nitrogen and phosphorus in the N–E Atlantic and the N–W Mediterranean with particular reference to non-refractory fractions and degradation, Deep Sea Res. I 51 (2004) 1975–1999.
[15] T. Serra, T. Granata, J. Colomer, A. Stips, F. Møhlenberg, X. Casamitjana, The role of advection and turbulent mixing in the vertical distribution of phytoplankton, Estuarine Coastal Shelf Sci. 56 (2003) 53–62.
[16] T. Serra, J. Colomer, C. Baserba, M. Soler, X. Casamitjana, Quantified of distribution of diatoms during the stratified period of Boadella reservoir, Hydrobiologia 489 (2002) 235–244.
[17] J. Vidal, X. Casamitjana, J. Colomer, T. Serra, The internal wave field in Sau Reservoir observation and working and modelling of third vertical mode, Limnol. Oceanogr. 50(4) (2005) 1326–1333.
[18] R. Romero, J.P. Antenucci, J. Imberger, One and three dimensional biogeochemical simulations of two differing reservoirs, Ecol. Model. 174 (2004) 143–160.